ELSEVIER

Physica A 207 (1994) 271–279

PHYSICA A

Fractal vortices in disordered superconductors

A. Raboutou, P. Peyral, C. Lebeau, J. Rosenblatt, J.P. Burin, Y. Fouad

Laboratoire de Physique des Solides, URA 786 au C.N.R.S., I.N.S.A., B.P. 14A, F-35043 Rennes Cedex, France

Abstract

We measure the low-frequency magnetic response $\chi = \chi' + i\chi''$ of halogenated ceramics $YBa_2Cu_3O_{7-\delta}F_x$ as functions of x, AC field amplitude H_0 and temperature T. The field of first flux penetration displays scaling behaviour: $H_1(x, T) = H_1(x, 0)\,(1 - T/T_c)^{\zeta}$, with T_c the coherence temperature and $\zeta = 2.7 \pm 0.2$; in all cases $H_1 \ll H_{c1}$ expected for the ideal material. A model where deviations from stoichiometry are assumed to result in local critical temperatures $T_c(\boldsymbol{r})$, is described. Superconductivity is due to regions where $T < T_c(\boldsymbol{r})$ with concentration $p(T)$. The coherence temperature is defined by $p(T_c) = p_c$, the percolation threshold. Critical exponents appear to be related to percolation exponents, in particular $\nu = 2\nu_p/3\beta_p \cong 1.33$, in agreement with the experimental value found in granular superconductors. Expressions are found for the magnetic fields observed in Euclidean space while being due to currents restricted to fractal percolation clusters. The free energy of the resulting fractal vortices accounts for the experimental value of the exponent in the temperature dependence of $H_1(T)$.

1. Introduction

It has been known for quite a long time that type II superconductors in a magnetic field H remain in the Meissner state (complete flux exclusion) up to a threshold field $H_{c1}(T)$. This corresponds to the Gibbs free energy being the same in the states with total magnetic flux $\Phi = 0$ and $\Phi = \Phi_0 = \pi\hbar/e$ in an infinite sample. One gets (see for example [1])

$$H_{c1} = \frac{F_1}{L\Phi_0} = \frac{\Phi_0}{4\pi\lambda_s^2\mu_0}\ln\left(\frac{\lambda_s}{\xi_s}\right), \tag{1}$$

where F_1 is the energy of a length L of the vortex line and λ_s and ξ_s are the bulk superconducting penetration depth and coherence length, respectively. When the

0378-4371/94/$07.00
SSDI 0378-4371(93)E0556-T

surface of the sample is taken into account one is led to introduce a second characteristic field for flux penetration,

$$H_s = \frac{\Phi_0}{4\pi\lambda_s \xi_s \mu_0} . \tag{2}$$

Its physical origin is the free-energy barrier opposing flux entrance due to the attraction between the vortex and its image across the surface. The barrier disappears for $H > H_s$. Although for $\lambda_s \gg \xi_s$, H_s may be well above H_{c1}, it is rather hard to observe because surface irregularities on the scale of λ_s are quite common in usual samples.

Shortly after the discovery of high T_c superconductors [2] it became clear that the actual field of first flux penetration was much smaller than the values predicted by Eqs. (1) or (2) [3,4]. This fact is usually ascribed to granularity [4–10], i.e. the condition of samples formed of grains all having the same critical temperature and coupled to their neighbours through random weak links of Josephson energies $J(\boldsymbol{r})$. We refer to this as mesoscopic disorder. Intergranular vortices would then enter the sample at fields $H_1(T)$ characteristic of Josephson junctions, giving $H_1 \ll H_{c1}$. In what follows we study a different (microscopic) type of disorder, obtained by partial halogenation of oxygen vacancies in superconducting ceramics. We also present a fractal cluster model which accounts for the experimental results on the temperature dependence of $H_1(T)$ and gives some insight on the analogies between granular and other types of disorder.

2. Experimental

Ceramic samples of chemical composition $YBa_2Cu_3O_{7-\delta}F_x$ have been prepared in the Laboratoire de Chimie du Solide et Inorganique Moléculaire, Université de Rennes, following a procedure described in [11]. A nominally stoichiometric ceramic $\delta = 0$, $x = 0$, where disorder is usually expected to be only mesoscopic, serves as a reference to be compared with the $\delta = 0.3$, $0 \leq x \leq 0.14$ samples. Neutron diffraction experiments [12] have shown that for this range of concentration fluorine atoms occupy vacant $(0\ \frac{1}{2}\ 0)$ sites, i.e. along the b-axis of the Perovskite structure.

We measure the response of a coil closely wound around the cylindrical sample to an ac field of amplitude H_0. The earth field is reduced to about 10^{-7} T by suitable μ-metal shielding. If vortices sweep across the sample against viscous forces, dissipation will show up via the imaginary part of the susceptibility χ''. Fig. 1a shows qualitatively the features of the Gibbs free energy in a homogeneous superconductor, leading to Eqs. (1) and (2). Energy barriers oppose the entrance of the first vortex into the volume of a large superconductor for $H < H_{c1}$ and across the surface of a finite sample for $H < H_s$. The absence of flux motion

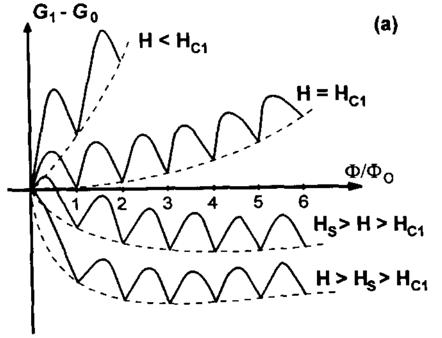

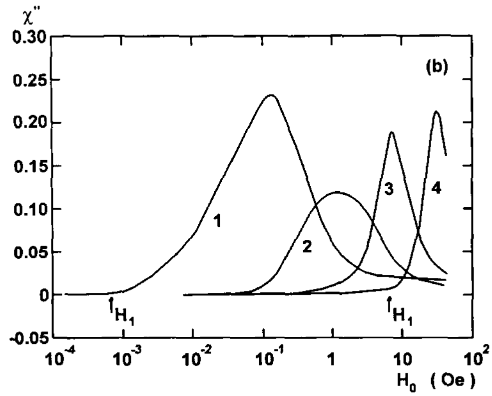

Fig. 1. (a) Schematic behaviour of the Gibbs free-energy difference as a function of the number of vortices inside the sample with (full line) and without (dotted line) a surface energy barrier, for different values of the applied field. Pinning is not taken into account. The increase of G for $\Phi > \Phi_0$ reflects the repulsive interaction between vortices. (b) Imaginary part of the susceptibility, associated to energy dissipation by flux motion in samples of $YBa_2Cu_3O_{7-\delta}F_x$. Curve 1, $\delta = x = 0$, $T = 90\,K$. Curve 2, $\delta = 0.3$, $x = 0.14$, $T = 4.2\,K$. Curve 3, $\delta = 0.3$, $x = 0.03$, $T = 4.2\,K$. Curve 4, $\delta = x = 0$, $T = 30\,K$. The arrows indicate the fields of first flux penetration.

$(\chi'' = 0)$ for $H < H_1$ displayed by the experimental data of Fig. 1b apparently confirms this picture, provided H_1 is identified with the field at which either the volume or the surface barrier disappears. But the temperature dependence of H_1 can be very well fitted by the law (Fig. 2)

$$H_1(T, x) = H_1(0, x)\,\varepsilon^{\zeta}\,, \qquad \zeta = 2.7\,, \tag{3}$$

with $\varepsilon = 1 - T/T_c$, while the Ginzburg–Landau description of λ_s and ξ_s gives $H_{c1} \propto H_s \propto \varepsilon$. Here the coherence temperature T_c is defined experimentally by a sharp increase on $\chi''(T)$ as the temperature decreases. Our group has reported on the critical behaviour of the intergranular penetration depth $\lambda \sim \varepsilon^{-\beta}$ and correlation length $\xi \sim \varepsilon^{-\nu}$ [13] (i.e. the range of the correlation function $S(\boldsymbol{r} - \boldsymbol{r}') = \langle \exp \mathrm{i}[\varphi(\boldsymbol{r}) - \varphi(\boldsymbol{r}')]\rangle - |\langle \exp \mathrm{i}\varphi \rangle|^2$ where $\varphi(\boldsymbol{r})$ is the superconducting phase at point $\boldsymbol{r}$), in connection with three-dimensional weak link arrays. We have found $\beta \cong 0.7$ and $\nu \cong 1.33$. Even when the replacements $\lambda_s \mapsto \lambda$, $\xi_s \mapsto \xi$ are tentatively made in Eqs. (1) and (2) one does not find the temperature dependence displayed in Eq. (3).

Characteristic parameters of our samples are given in Table 1. Again, taking accepted values $\lambda_s(0) \cong 150\,\mathrm{nm}$, $\xi_s(0) \cong 0.5\,\mathrm{nm}$, one is far from obtaining an order-of-magnitude agreement between $H_{c1}(0)$ or $H_s(0)$ with the extrapolated experimental values of $H_1(0)$. A similar situation is found in weakly coupled granular superconductors [13], where similarly to the data in Fig. 1b, very low values of the excitation field are need for an accurate description of $H_1(T)$ over a large temperature range.

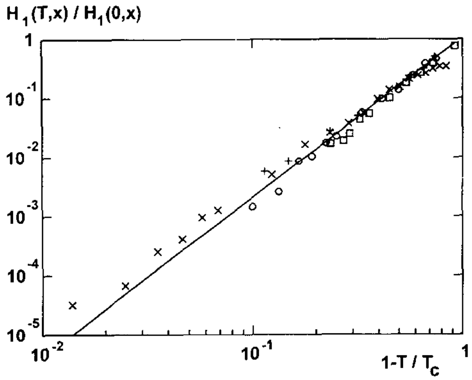

Fig. 2.

Table 1
Characteristic parameters of $YBa_2Cu_3O_{7-\delta}F_x$ samples.

δ	x	T_c (K)	$H_1(0)$ (Oe)
0	0	91.3	21.5
0.3	0	60.0	1.32
0.3	0.03	58.7	0.49
0.3	0.14	54.9	0.093

Fig. 2. Scaling-like behaviour of the field of first flux penetration into fluorinated ceramics: (×) $\delta=0$, $x=0$; (○) $\delta=0.3$, $x=0$; (+), $\delta=0.3$, $x=0.03$; (□) $\delta=0.3$, $x=0.14$. The straight line has slope 2.7.

3. The model

Our experimental results suggest that first flux penetration is governed by the same physical phenomenon – free-energy barriers – in both homogeneous and disordered superconductors, although displaying widely different temperature dependences. On the other hand, granularity and doping (i.e. mesoscopic and microscopic disorder respectively) induce similar behaviours. The following subsections show that the same exponents are indeed expected for both types of disorder but they should differ from those in the homogeneous case.

3.1. Disordered superconductors

In cuprates, the smallness of $\xi_s(T)$ suggests that inevitable deviations from stoichiometry result in spatial fluctuations of the critical temperature, $T_c(\boldsymbol{r})$, defined over regions of typical size $a > \xi_s$, hereinafter taken as a microscopic unit of length. We define $\varepsilon(\boldsymbol{r}) = [T - T_c(\boldsymbol{r})]/T_c$, $\Delta\varepsilon(\boldsymbol{r}) = \varepsilon(\boldsymbol{r}) - \varepsilon = [T_c(\boldsymbol{r}) - T_c]/T_c = \Delta T_c(\boldsymbol{r})/T_c$ and the correlation function

$$K(\boldsymbol{r}-\boldsymbol{r}') = \langle \Delta\varepsilon(\boldsymbol{r}')\,\Delta\varepsilon(\boldsymbol{r})\rangle_{\mathrm{d}} = \langle \Delta T_c(\boldsymbol{r})\,\Delta T_c(\boldsymbol{r}')\rangle_{\mathrm{d}}/T_c^2\,. \tag{4}$$

Disorder in $T_c(\boldsymbol{r})$ will be irrelevant [14] if, in a volume $\xi^d \to \infty$ as $T \to T_c$,

$$\langle \Delta\varepsilon^2\rangle_d = \xi^{-2d}\sum_{rr'} K(\boldsymbol{r}-\boldsymbol{r}') < \varepsilon^2 = \left(\frac{\xi}{\xi(0)}\right)^{-2/\nu}\,. \tag{5}$$

For $K(\boldsymbol{r}-\boldsymbol{r}') \propto \delta_{rr'}$, i.e. uncorrelated disorder, we obtain the original Harris criterion [15] for irrelevance of disorder, namely $d\nu - 2 \geqslant 0$ in the homogeneous system. However, in our case, a screening supercurrent will be able to circulate between two points only if they are connected by a continuous path where

$T_c(\boldsymbol{r}) > T$. The probability $p(T)$ that a region of size a centred around $\boldsymbol{r}$ has $T_c(\boldsymbol{r}) > T$, is the parameter of a temperature-dependent percolation problem, with correlation length $\xi_p \approx |1 - p/p_c|^{-\nu_p}$. Conversely, the thermal phase–phase correlation function $S(\boldsymbol{r} - \boldsymbol{r}') \neq 0$ only if $\boldsymbol{r}$ and $\boldsymbol{r}'$ are connected, that is they belong to the same percolation cluster. It is therefore plausible to assume that its range, $\xi(T) \sim \varepsilon^{-\nu}$ varies like ξ_p, i.e. $|1 - p/p_c| \approx \varepsilon^{\nu/\nu_p}$ irrespective of the particular distribution of T_c's in each sample.

Long-range phase coherence and thereby infinite conductivity and perfect diamagnetism appear at $T \to T_c^+$ $(p \to p_c^-)$ when the infinite cluster is formed. The latter is known to have the same structure as large but finite clusters near p_c [16], in particular the pair connectedness $C(r) \sim 1/r^{d-2+\eta_p} = r^{-2\tilde{\beta}_p}$ ($\tilde{\beta}_p = \beta_p/\nu_p$ is a quotient of percolation exponents). We can now write the function $K(0, \boldsymbol{r})$ as being proportional to the probability p that the origin belongs to a cluster, that it is the infinite one ($P_\infty \approx \xi_p^{-\tilde{\beta}_p}$), and to the probability that the site at $\boldsymbol{r}$ belongs to the same cluster, $C(r)$. Finally, summing over a volume ξ^d:

$$\sum_r K(0, \boldsymbol{r}) \approx p\, P_\infty \sum_r C(r) \approx \xi^{d-3\tilde{\beta}_p}\,, \qquad (6)$$

while a similar dependence on ξ is obtained for the number of pairs in finite clusters. After replacing Eq. (6) into Eq. (5) the condition for irrelevance of disorder becomes

$$\langle \Delta\varepsilon^2 \rangle_d / \varepsilon^2 \approx \xi(0)^{-2/\nu} \xi^{-(d-2/\nu)} \sum_r K(0, \boldsymbol{r}) \approx \xi(0)^{-3\tilde{\beta}_p} \varepsilon^{3\tilde{\beta}_p \nu - 2} < +\infty \qquad (7)$$

implying $3\tilde{\beta}_p \nu - 2 \geq 0$ [14]. This condition is definitely not satisfied by $d = 3$ homogeneous systems belonging, like superconductivity, to the XY class of universality. Disorder is therefore relevant and new exponents are expected. Now condition (7) is just a special case of an extended Harris criterion [14], which, in our case, leads to $\nu = 2/3\tilde{\beta}_p \cong 1.33$. This is the value found in experiments on granular material. Indeed, a very similar reasoning, where the intergranular coupling energy $J(\boldsymbol{r})$ replaces $T_c(\boldsymbol{r})$ [17], has been shown to lead to the same value of ν. We have thus justified the equivalence between mesoscopic and microscopic disorder in cuprates.

3.2. *Fractal electrodynamics*

Percolation clusters are known to be fractals, with a characteristic dimension $D_p = d - \tilde{\beta}_p \cong 2.5$ [16] and a backbone dimension $D_b \cong 2$ [18]. Then the arguments developed in the preceding subsection raise naturally the following question: what fields are seen in d-dimensional space while being due to currents in D dimensions $(D < d)$? Our heuristic answer is based on the simple idea that fractal and Euclidean observers see the same total amount of an extensive quantity F defined on a region of size L in a fractal $\mathscr{F}$ but they refer it to volumes L^D and L^d and therefore measure different densities. In a volume element $\mathrm{d}^D\boldsymbol{r}$, Fractalians see a slowly varying density per site $f_D(\boldsymbol{r})$, but Euclideans would reckon a wildly varying function in the corresponding volume $\mathrm{d}^d\boldsymbol{r}$, namely $f_D(\boldsymbol{r})\, w(\boldsymbol{r})$. Here the indicator $w(\boldsymbol{r}) = 1$ if $\boldsymbol{r} \in \mathcal{F}$, $w(\boldsymbol{r}) = 0$ if $\boldsymbol{r} \notin \mathcal{F}$ and distances are measured in units of a. Thus both observers measure the same total current, magnetic flux, etc., but different current densities, induction, etc. In general the euclidean density will be a continuous function $f(\boldsymbol{r})$ such that (lengths are measured in units of a)

$$F = \int f(\boldsymbol{r})\, \mathrm{d}^d\boldsymbol{r} = \int f_D(\boldsymbol{r})\, \mathrm{d}^D\boldsymbol{r} = \int f_D(\boldsymbol{r})\, w(\boldsymbol{r})\, \mathrm{d}^d\boldsymbol{r} = \int f_D(\boldsymbol{r}) \langle w \rangle_d\, \mathrm{d}^d\boldsymbol{r}\,. \tag{8}$$

The mean value theorem has been used in the last step. We define a dilution factor

$$W(L) = \langle w \rangle_d = \begin{cases} (a/L)^{d-D} & \text{if } a \leqslant L < \xi(T)\,, \\ (a/\xi)^{d-D} & \text{if } L > \xi(T)\,, \end{cases} \tag{9}$$

which depends on the domain of integration. We thus get the transformation rules

$$f_D(\boldsymbol{r}) \mapsto f(\boldsymbol{r}) = W f_D(\boldsymbol{r})\,, \qquad \mathrm{d}^D\boldsymbol{r} = W\, \mathrm{d}^d\boldsymbol{r}\,, \tag{10}$$

which apply immediately to the 2D densities, mesoscopic induction $\boldsymbol{b} = W\boldsymbol{b}_D$ and current density $\boldsymbol{j} = W\boldsymbol{j}_D$. It seems natural now to postulate the formal validity of Maxwell's equation in fractal space. For example, 3D magnetic energy density $b^2/2\mu = W b_D^2/2\mu_D$, which requires the definition of a fractal permeability $\mu_D = \mu/W$. Similarly,

$$\boldsymbol{j} = \frac{\boldsymbol{\nabla} \wedge \boldsymbol{b}}{\mu} = W\boldsymbol{j}_D = W\, \frac{\boldsymbol{\nabla}_D \wedge \boldsymbol{b}_D}{\mu_D} \tag{11}$$

introduces the differential operator $\boldsymbol{\nabla}_D = W^{-1}\boldsymbol{\nabla}$. While the divergence operator in ordinary space transforms a two-dimensional vector density into a three-dimensional density, the operator $\boldsymbol{\nabla}_D \cdot$ applied to the same density results in a new D-dimensional density. Thus the divergence theorem is written symbolically $\int \mathrm{d}^D\boldsymbol{r}\, \boldsymbol{\nabla}_D \cdot = \oint \mathrm{d}^{d-1}\boldsymbol{r}\, \boldsymbol{n} \cdot = W^{-1} \oint \mathrm{d}^{D-1}\boldsymbol{r}\, \boldsymbol{n} \cdot$, where $\boldsymbol{n}$ is a vector perpendicular to the surface of dimension $d-1$ and therefore also to the intersection (of dimension $D-1$) of this surface with the fractal. Using this operator, the kinetic energy of the currents has a density $\lambda^2 |\boldsymbol{\nabla} \wedge \boldsymbol{b}|^2/2\mu = W\lambda_D^2 |\boldsymbol{\nabla}_D \wedge \boldsymbol{b}_D|^2/2\mu_D$, where $\lambda_D = W\lambda$ is just the measure of the intersection of the fractal with a segment of length equal to the penetration depth λ.

One can now calculate the threshold fields for single-vortex penetration in the infinite cluster. We observe from Eq. (1) that $H_{c1}\Phi_0$ is a linear density of energy in a homogeneous system. Its fractal counterpart will be affected, according to Eqs. (9) and (10), by a temperature-dependent factor $W(\xi)$ for $L > \xi$, which may explain the unexpected temperature dependence of $H_1(T)$.

In order to see this in more detail, we retrace the steps (in D dimensions) of the classical calculation [1] leading to H_{c1} and H_s. As suggested by Fig. 1a, at H_{c1} the Gibbs free energies $G_0 = G(\Phi = 0)$ and $G_1 = G(\Phi = \Phi_0) = G_0 + F_1(\Phi_0, L) -$

$H\Phi_0 L$ are equal. The free energy F_1 is a sum of kinetic and magnetic energies, whose minimisation gives London's equation

$$\boldsymbol{b}_D + \lambda_D^2 \boldsymbol{\nabla}_D \wedge \boldsymbol{\nabla}_D \wedge \boldsymbol{b}_D = 0 \tag{12}$$

in the fractal, and its analogue in 3D. The vortex solution has a logarithmic singularity on the axis, $\boldsymbol{b} \cong (\Phi_0/2\pi\lambda^2)\ln(\lambda/r)$ in cylindrical coordinates. Taking into account Eq. (12) and known vector identities, one obtains [1]

$$\begin{aligned} F_1(L) &= \int \mathrm{d}^D \boldsymbol{r}\, \boldsymbol{\nabla}_D \cdot (\boldsymbol{b}_D \wedge \boldsymbol{\nabla}_D \wedge \boldsymbol{b}_D) \frac{\lambda_D^2}{2\mu_D} = \int \mathrm{d}^{D-1} \boldsymbol{r}\, \boldsymbol{n} \cdot (\boldsymbol{b} \wedge \boldsymbol{\nabla} \wedge \boldsymbol{b}) \frac{\lambda^2}{2\mu W(a)} \\ &= \int \mathrm{d}^{D-1} \boldsymbol{r} \frac{\Phi_0^2}{4\pi\lambda^2\mu} \ln\left(\frac{\lambda}{a}\right) = LW(L) \frac{\Phi_0^2}{4\pi\lambda^2\mu} \ln\left(\frac{\lambda}{a}\right). \end{aligned} \tag{13}$$

The second integral results from the transformation rules and the divergence theorem. The domain of integration is a cylinder of length $L > \xi$ along the z-axis and radius a, resulting in $W(a) = 1$. Finally, from the condition $G_1 = G_0$,

$$H_{c1} = \frac{F_1}{L\Phi_0} = \left(\frac{a}{\xi}\right)^{d-D} \frac{\Phi_0}{4\pi\lambda^2\mu} \ln\left(\frac{\lambda}{a}\right) \approx \varepsilon^{(d-D)\nu + 2\beta}. \tag{14}$$

If $H_1(T) = H_{c1}$ the exponent should be made equal to $\zeta \cong 2.7$. Now, the preceding subsection showed that exponents found on granular material should apply also to microscopic disorder. When the known values of ν and β are replaced in (14), one finds $D \cong D_b \cong 2$, i.e. the backbone dimensionality. This means that deep inside the sample only closed loops in the fractal allow the circulation of screening currents.

The sample surface, or rather its intersection with the infinite cluster, is taken into account through the addition of an image antivortex to the vortex solution of Eq. (12). We skip the details of the calculation which closely follows the classical one [1], and just point out that G has a maximum at fixed field when the distance x_m between the vortex and the surface is

$$x_m = \frac{\Phi_0}{2\pi\lambda\mu H} \frac{W(\xi)}{1 + W(\xi)}. \tag{15}$$

Actually $H(x_m)$ is bounded by the well-known Silsbee rule [19], namely that the current crossing the segment x_m between the vortex and the surface should be below critical. For the critical current the phase gradient is of order $1/\xi(T)$ [20]. The total phase change around the vortex core is 2π. Since inside the sample the current circulates over a characteristic distance λ, the average phase gradient is of order $2\pi/2\pi\lambda = 1/\lambda$. The same current is squeezed across x_m near the boundary, so its density increases by a factor λ/x_m, the phase gradient becoming $1/x_m$. The current is below critical if $x_m > \xi(T)$. This gives

$$H_s = \frac{\Phi_0}{4\pi\lambda\xi\mu} \frac{W(\xi)}{1 + W(\xi)} \approx \varepsilon^{(d-D+1)\nu + \beta}. \tag{16}$$

Replacing $D = D_p = d - \tilde{\beta}_p$, $\nu = 2/3\tilde{\beta}_p$ and $\beta \cong 0.7$ one obtains $\zeta = \beta + 2(1 + \tilde{\beta}_p)/3\tilde{\beta}_p = 2.7$, in very good agreement with experiment. This may still be compatible with the arguments given after Eq. (14). Vortex–antivortex interactions are surely dependent on the properties of space between them; in this sense dead ends and the dimension D_p may become relevant.

4. Discussion

Which field is actually measured, H_{c1} or H_s? A definite answer to this question would require an independent measurement of $\lambda(T)$, which is beyond the scope of this paper. The existence of these two fields nevertheless should be expected on very general grounds. Our data show that both have the same temperature dependence, as is the case of classical superconductors, which obey, however, a different power law. Indeed, with reference to Fig. 2, the fit to the power law (3) extends for about five decades in $H_1(T)/H_1(0)$. In principle $H_s \gg H_{c1}$, but a crossover between the two would probably have appeared in this interval if the two fields had different behaviours.

As said before, the observation of the field H_s is not easy in classical superconductors, because it requires a sample surface smooth on the scale of λ_s (typically 50 to 100 nm). For the infinite cluster discussed here, the surface is itself a fractal on the scale of $\xi \ll \lambda$ but should become smooth on the mesoscopic scale λ.

Finally our model not only correctly describes the observed temperature dependence of the first penetration field in high temperature superconductors, but gives a possible explanation (through the factor $W < 1$) for the weak fields encountered in practice. It also accounts for similarities in the effects of different types of disorder.

References

[1] P.G. de Gennes, Superconductivity of Metals and Alloys (Benjamin, New York, 1966).
[2] J.G. Bednorz and K.A. Muller, Z. Phys. B 64 (1986) 189.
[3] A.P. Malozemoff, in: Physical Properties of High Temperature Superconductors, D.M. Ginsberg, ed. (World Scientific, Singapore, 1989) p. 73, and references therein.
[4] P. Peyral, J. Rosenblatt, A. Raboutou, C. Lebeau, C. Perrin, O. Peña, A. Perrin and M. Sergent, Physica C 153–155 (1988) 1493.
[5] G. Deutscher and K.A. Müller, Phys. Rev. Lett. 59 (1987) 1745.
[6] J.R. Clem, Physica C 153–155 (1988) 50.
[7] A. Giannelli and C. Giovannella, J. Less Common Met. 164–165 (1990) 1488.
[8] S.L. Shindé, J. Morill, D. Goland, D.A. Chance and T. McGuire, Phys. Rev. B 41 (1990) 8838.
[9] B. Schulz, B. Schliepe, W. Wisny and K. Baberschke, Solid State Commun. 80 (1991) 111.
[10] W.H. Tierman and R.B. Hallock, Phys. Rev. B 46 (1992) 3688.

[11] C. Perrin, O. Peña, M. Sergent, P. Christensen, G. Fonteneau and J. Lucas, Supercond. Sci. Technol. 2 (1989) 35.
[12] C. Perrin, A. Dinia, O. Peña, M. Sergent, P. Burlet and J. Rossat-Mignod, Solid State Commun. 76 (1990) 401.
[13] A. Raboutou, J. Rosenblatt and P. Peyral, Phys. Rev. Lett. 45 (1980) 1035.
[14] A. Weinrib and B.I. Halperin, Phys. Rev. B 27 (1983) 413.
[15] A. Brooks Harris, J. Phys. C 7 (1974) 1671.
[16] See for example D. Stauffer, Phys. Rep. 54 (1979) 1;
J.W. Essam, Rep. Prog. Phys. 43 (1980) 53.
[17] J. Rosenblatt, P. Peyral, A. Raboutou and C. Lebeau, Physica B 152 (1988) 100.
[18] Y. Gefen, A. Aharony, B.B. Mandelbrot and S. Kirkpatrick, Phys. Rev. Lett. 47 (1981) 1771.
[19] F.B. Silsbee, J. Wash. Acad. Sci. 6 (1916) 597.
[20] J. Rosenblatt, in: Percolation, Localisation and Superconductivity, NATO ASI Series, A.M. Goldman and S.A. Wolf, eds. (Plenum, New York, 1984) p. 431.